97-GT-397

THE AMERICAN SOCIETY OF MECHANICAL ENGINEERS
345 E. 47th St., New York, N.Y. 10017

~~96-GT-397~~

The Society shall not be responsible for statements or opinions advanced in papers or discussion at meetings of the Society or of its Divisions or Sections, or printed in its publications. Discussion is printed only if the paper is published in an ASME Journal. Authorization to photocopy material for internal or personal use under circumstance not falling within the fair use provisions of the Copyright Act is granted by ASME to libraries and other users registered with the Copyright Clearance Center (CCC) Transactional Reporting Service provided that the base fee of $0.30 per page is paid directly to the CCC, 27 Congress Street, Salem MA 01970. Requests for special permission or bulk reproduction should be addressed to the ASME Technical Publishing Department.

Copyright © 1997 by ASME All Rights Reserved Printed in U.S.A

DIRECT FULL SURFACE SKIN FRICTION MEASUREMENT USING NEMATIC LIQUID CRYSTAL TECHNIQUES

BREAK

D. R. Buttsworth, S. J. Elston, and T. V. Jones

Department of Engineering Science, University of Oxford

Parks Road, Oxford, United Kingdom

ABSTRACT

New techniques for the direct measurement of skin friction using nematic liquid crystal layers are demonstrated. Skin friction measurements can be made using a molecular rotation time technique or an equilibrium orientation technique. A mathematical model describing the molecular dynamics of the nematic liquid crystal layer has been introduced. Theoretical results from the proposed mathematical model are in excellent agreement with the current experimental measurements. It is thus demonstrated that the present model captures the essential physics of the nematic liquid crystal measurement techniques. Estimates based on the variance of the liquid crystal calibration data indicate that skin friction measurements to within ± 4 % should certainly be possible. The techniques offer the considerable advantage of simplicity, without any compromise on the accuracy, relative to other surface shear stress measurement techniques. The full surface measurement capacity of the equilibrium orientation technique is demonstrated by measuring the skin friction distribution around a cylindrical obstruction in a fully developed laminar flow.

NOMENCLATURE

- a duct height
- b duct width
- c function of du/dy, tilt angle, and viscosity coefficients. (Pa)
- C nondimensional value of c, cl^2/K
- K elastic constant (N)
- l thickness of liquid crystal layer
- n dummy variable used in summation (in Eq. 5)
- Δn birefringence
- p pressure (Pa)
- t time, usually measured relative to the air flow start or stop
- T nondimensional time, $Kt/\mu l^2$
- u velocity
- x streamwise coordinate (in the direction of the duct length)
- y vertical coordinate (in the direction of the duct height)
- Y nondimensional distance through layer, y/l
- z transverse coordinate (in the direction of the duct width)
- θ angle of liquid crystal director
- λ wavelength of light
- μ dynamic viscosity (Pa.s)
- ν kinematic viscosity, μ/ρ ($m^2.s^{-1}$)
- ρ density ($kg.m^{-3}$)
- σ standard deviation
- τ_w skin friction (surface shear stress) (Pa)

subscripts

- 1, 3 elastic constants for the liquid crystal material
- 63.2 time constant based on an angle change of $(1-e^{-1}) \times 100$ %
- 10-90 rotation time based on intensity change between 10 and 90 %

INTRODUCTION

Skin friction (otherwise known as surface shear stress) is a key parameter of interest in both fundamental and applied aerodynamics investigations. Skin friction measurements can provide an insight into the physics of complex flow fields, and can also identify the contribution of the viscous drag to the overall loss production in aerodynamic configurations. Furthermore, skin friction measurements can also be used to validate computational fluid dynamics predictions.

It is therefore not surprising that many skin friction measurement techniques have already been developed. Detailed reviews of these methods can be found elsewhere (Winter, 1977; Fernholz et al., 1996; Hanratty and Campbell, 1996). Briefly however, the majority of the previous methods are *indirect* techniques in that a parameter other than the skin friction (e.g., heat transfer) is

Presented at the International Gas Turbine & Aeroengine Congress & Exhibition
Orlando, Florida — June 2–June 5, 1997
This paper has been accepted for publication in the Transactions of the ASME
Discussion of it will be accepted at ASME Headquarters until September 30, 1997

Downloaded From: http://proceedings.asmedigitalcollection.asme.org/ on 05/24/2018 Terms of Use: http://www.asme.org/about-asme/terms-of-use

actually measured. Indirect techniques then rely on assumptions which relate the measured parameter to the skin friction. *Direct* skin friction measurement techniques avoid such assumptions, and are therefore to be preferred, particularly in complex flows where these assumptions break down. Direct methods include floating element (Marshakov et al., 1996), oil film (Tanner and Blows, 1976; Bandyopadhyay and Weinstein, 1991), and liquid crystal techniques (Bonnet et al., 1989; Reda et al., 1994, 1996). Of these techniques, only the liquid crystal method described by Reda et al. (1996), which relys on the color change response of cholesteric liquid crystal, has been developed to give quantitative *full surface* skin friction measurements. However, the physics of this liquid crystal technique is not well understood, and furthermore, the practical implementation of this technique is very complicated.

The focus of the current paper is a simple and direct full surface skin friction measurement technique that utilizes the wave guiding properties of nematic liquid crystals (e.g., Walton, 1990; Jones and Walton, 1991; Jones, 1992). With the nematic liquid crystal skin friction method, a surface layer of nematic liquid crystal is initially aligned approximately perpendicular to the anticipated flow direction. The application of the flow causes the molecules to rotate forming a twisted structure which alters the orientation of the polarized light that is transmitted through the layer. Walton (1990) found that the rotation time of the nematic liquid crystal (as indicated by the rise time of the transmitted light intensity) varies inversely with the applied shear stress. In subsequent investigations, it was found that, under relatively low shear stress conditions, the liquid crystal director at the fluid interface did not fully align with the flow direction, but adopted an equilibrium orientation that was also a function of the applied shear stress. Neither the rotation time technique nor the equilibrium orientation technique has yet been applied or developed to full potential. Therefore, the aim of the present work is to extend the development of these nematic liquid crystal techniques and demonstrate the potential for skin friction measurements.

NEMATIC LIQUID CRYSTAL TECHNIQUE

General Arrangement

The liquid crystal layer is prepared by first painting polyvinyl alcohol (PVA) onto the surface of interest (usually perspex or glass). Once the PVA is dry, the layer is unidirectionally rubbed with a velvet cloth. The PVA is rubbed at an angle roughly perpendicular to the anticipated flow direction. It appears probable that this rubbing process aligns the long polymer molecules at the PVA surface with the stroke direction through a localized melting and shearing process. Nematic liquid crystals are then painted onto the surface. The surface treatment of the PVA layer causes the nematic liquid crystal molecules, being relatively long rod-like molecules, to align with the direction of the rubbing. In the absence of external forces, the liquid crystal director throughout the entire thickness of the layer, thus lies approximately parallel to the direction in which the PVA layer was rubbed. (The director indicates the mean molecular orientation, i.e., the direction of the "rod".)

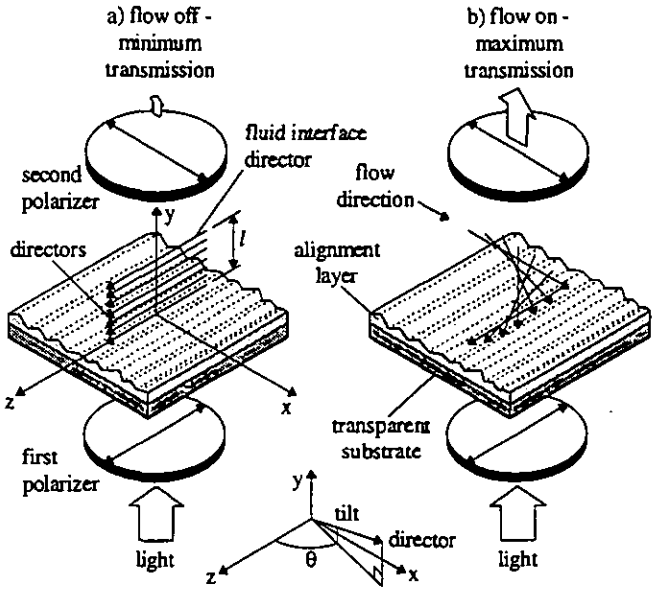

Figure 1. Illustration of the liquid crystal technique.

A schematic illustration of the nematic liquid crystal skin friction technique is given in Fig. 1. Plane polarized light with an orientation parallel to the surface alignment direction passes though the liquid crystal layer and, provided the flow has not yet been initiated, the light also passes through the liquid crystal layer with minimal distortion. The liquid crystal is viewed through another polarizer that is usually oriented perpendicular to the polarization plane of the illumination light. When the flow is initiated, the molecules attempt to align with the flow direction, but because the molecules are strongly anchored at the solid interface by the surface treatment, a twisted structure forms. Because the liquid crystal layer is much thicker than the wavelength of the polarized light, the twisted layer is able to guide the plane of polarization of the light through the twisted structure. As the liquid crystal layer reorients due to the applied shear stress, a change in transmitted light intensity can be observed through the second polarizer.

Streamwise Layer Motion

When a shear stress is suddenly applied to the exposed surface of the liquid crystal, the layer attempts to move in the direction of the applied shear. For a layer of sufficient thickness, the streamwise acceleration may be approximated by the diffusion equation for an isotropic fluid (White, 1991, p.149),

$$\frac{\partial^2 u}{\partial y^2} = \frac{1}{\nu}\frac{\partial u}{\partial t} \tag{1}$$

subject to the boundary and initial conditions,

$$\left(\frac{\partial u}{\partial y}\right)_{y=l} = \frac{\tau_w}{\mu} \quad \text{for } t > 0 \tag{2}$$

Downloaded From: http://proceedings.asmedigitalcollection.asme.org/ on 05/24/2018 Terms of Use: http://www.asme.org/about-asme/terms-of-use

$$u(0,t) = 0 \tag{3}$$

$$u(y,0) = 0 \tag{4}$$

The solution of this problem can be written (from the solution of an analogous heat transfer problem, Carslaw and Jaeger, 1959, p.113),

$$\frac{u}{\tau_w l/\mu} = \frac{y}{l} - \frac{8}{\pi^2}\sum_{n=0}^{\infty}\frac{(-1)^n}{(2n+1)^2}.e^{\frac{-(2n+1)^2\pi^2\nu t}{4\ l^2}}\sin\left(\frac{(2n+1)\pi}{2}\frac{y}{l}\right) \tag{5}$$

Equation (5) predicts that the velocity at the fluid interface (i.e., at $y = l$) is within 1 % of the steady value at a time give by,

$$t \approx 1.78\frac{l^2}{\nu} \tag{6}$$

Thus, at a similar time, the velocity distribution within the layer approaches the steady (linear) velocity profile,

$$u = \frac{\tau_w y}{\mu} \tag{7}$$

For the work described in the current paper, the kinematic viscosity of the liquid crystal was around 580×10^{-6} m^2.s^{-1} (at 20 °C), and the thickness of the layer is estimated to be around 10 μm. Thus, the steady velocity profile was set up in approximately 0.3 μs from of the application of the flow (using Eq. 6). In the present investigation, the molecular reorientation due to the applied shear stress was on the order of 1 s, and hence, the velocity profile establishment time in the liquid crystal layer is insignificant. The surface shear stresses generated in the present experiments were generally less than 4 Pa. Thus, the maximum surface velocity of the layer would have been around 7×10^{-5} m.s^{-1}, which is an insignificant fraction of the air flow velocities used in the present experiments (on the order of 10 m.s^{-1}). Hence, the downstream movement of the liquid crystals did not have a measurable effect on the surface shear stress generated by the air flow.

Molecular Rotation

The surface treatment orients the liquid crystal director perpendicular to the anticipated flow direction and anchors the liquid crystal molecules at the solid interface in that direction. Furthermore, the surface treatment also imparts a small azimuthal tilt angle (of around 3°) to the liquid crystal molecules (Fig. 1). The liquid crystal molecules rotate when a shear stress is applied to the fluid interface because the local gradient of streamwise velocity (du/dy) exerts a torque (in the θ direction) on the tilted molecule.

A simple model for the motion of the liquid crystal director can be written as.

$$\mu\frac{\partial\theta}{\partial t} = K\frac{\partial^2\theta}{\partial y^2} + c.\cos\theta \tag{8}$$

Equation (8) balances the viscous torque which retards the rotation of the molecules, against the elastic aligning torque, and a rotation forcing-function. The forcing-function ($c.\cos\theta$) is itself a function of the gradient of the streamwise velocity, the molecular tilt angle, and the various viscosities associated with the nonisotropic liquid crystal molecules. As it is presently assumed that the steady velocity profile within the liquid crystal layer is established rapidly and is also linear, the parameter c will be constant throughout the thickness of the layer and will be proportional to the applied shear stress (τ_w). In nondimensional form, Eq. (8) can be written,

$$\frac{\partial\theta}{\partial T} = \frac{\partial^2\theta}{\partial Y^2} + C.\cos\theta \tag{9}$$

where,

$$T = \frac{Kt}{\mu l^2} \tag{10}$$

$$Y = \frac{y}{l} \tag{11}$$

$$C = \frac{cl^2}{K} \tag{12}$$

For the present analysis, it is assumed that the molecules in contact with the solid interface are strongly anchored due to the surface alignment treatment, and that prior to the start of the flow, the liquid crystal director throughout the entire thickness of the layer is perpendicular to the flow direction. Furthermore, at the fluid interface, there is negligible torque. Thus, the appropriate boundary and initial conditions for Eq. (9) are,

$$\theta(0,T) = 0 \tag{13}$$

$$\left(\frac{\partial\theta}{\partial Y}\right)_{Y=1} = 0 \tag{14}$$

$$\theta(Y,0) = 0 \tag{15}$$

Solution of Eq. (9) was achieved using an explicit finite difference routine with 51 nodes distributed evenly throughout the layer. An investigation of solution convergence suggests that results obtained with this level of discretization are within approximately 1 % of the actual solution.

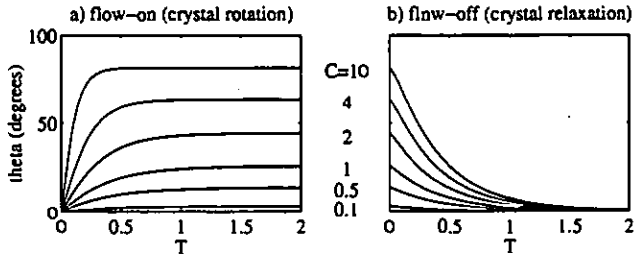

Figure 2. Theoretical prediction of the fluid interface director dynamics.

For rapidly established air flows, there will effectively be a step change in the value of C (at $T = 0$) when the flow is initiated (since C is proportional to the applied shear stress). For various steps in the value of C, results from the finite difference solution (at $Y = 1$) are given in Fig. 2a. (Provided the liquid crystal layer operates as a perfect wave guide, i.e., provided the twist is gentle relative to the wavelength of the light, it is the director orientation at the fluid interface, $Y = 1$, that determines the orientation of the transmitted light, and hence the intensity observed through the second polarizer.) For the same values of C, Fig. 2b presents results for the relaxation of

Downloaded From: http://proceedings.asmedigitalcollection.asme.org/ on 05/24/2018 Terms of Use: http://www.asme.org/about-asme/terms-of-use

the liquid crystal layer resulting from switching off the air flow, after the orientation of the liquid crystal layer has reached its steady state distribution. Results in Fig. 2b, were again obtained using the finite difference routine, however, this time, the initial conditions were given by the solution of,

$$\frac{\partial^2\theta}{\partial Y^2} = -C\cos\theta \qquad (16)$$

subject to the boundary conditions described by Eqs. (13) and (14). Equation (16) was integrated using a high-order Runge-Kutta method.

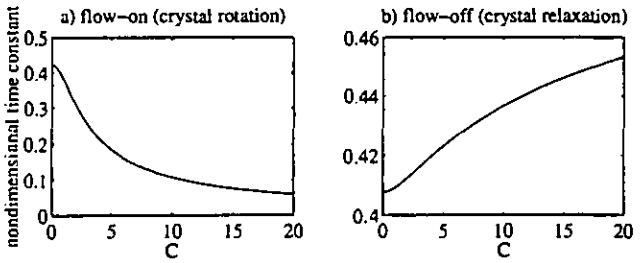

Figure 3. Theoretical prediction of the time constant for the fluid interface director dynamics.

For the flow-on and flow-off cases (Fig. 2, parts a and b) a nondimensional time constant was defined as the value of T at which the fluid interface director had changed its orientation by 63.2 % of its equilibrium value of θ. Results from this analysis of the theoretical model are given in Fig. 3 as a function of C (which is proportional to the applied shear stress). It is clear that the time constant associated with the flow on crystal rotation is a relatively strong function of the applied shear stress (Fig 3a), particularly in comparison to the flow-off crystal relaxation time constant (Fig 3b). The theoretical results in Fig. 3a describe the rotation time shear stress measurement technique originally investigated by Walton (1990). For $C > 10$ (approximately), the theoretical rise time varies approximately with the inverse of the applied shear stress. That is, the theoretical rotation time relationship can be approximated as,

$$T_{63.2} \propto \frac{1}{C} \qquad (17)$$

or, converting back to dimensional parameters,

$$t_{63.2} \propto \frac{\mu}{\tau_w} \qquad (18)$$

which indicates that the rotation time is also proportional to the material viscosity, but is independent of the elastic constant, and the layer thickness.

In Fig. 4, theoretical results are also given for the steady state orientation of the fluid interface director, based on the solution of Eq. (16). This figure describes the second nematic liquid crystal skin friction measurement technique, the equilibrium orientation technique. The theoretical results indicate that for shear stresses corresponding to values of $C < 10$ (approximately), the equilibrium orientation is a strong function of the applied shear stress. The equilibrium orientation technique offers advantages over the rotation time technique, in that there are no restrictions on the test flow establishment time. (For the rotation time technique, the test flow establishment time must be short relative to the rotation time constant of the liquid crystal layer.) However, with the equilibrium orientation technique, the measured intensity will be a function of the model illumination, and hence an in-situ illumination calibration will be necessary. Thus, in turn, the rotation time technique offers advantages over the equilibrium orientation technique in that the measured parameter (the orientation time) is independent of the absolute intensity of the light.

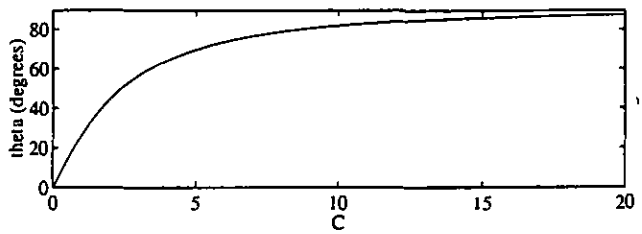

Figure 4. Theoretical prediction of the fluid interface equilibrium orientation.

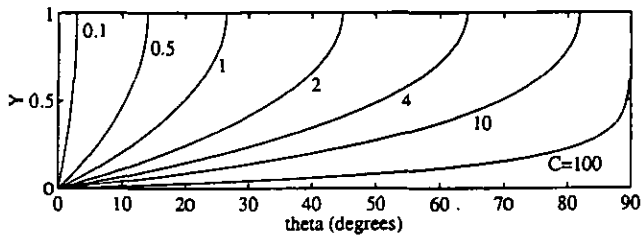

Figure 5. Theoretical prediction of the director orientation throughout the liquid crystal layer.

Results are presented in Fig. 5 for the equilibrium director orientation throughout the thickness of the layer (again from the solution of Eq. 16). Since the present layer thickness was around 10 μm, the effective pitch of the twisted nematic structure will be around 40 μm (since there is approximately a quarter of a twist within the layer). For good wave guiding, a pitch significantly greater than $\lambda/\Delta n$ is generally required. Assuming λ = 500 nm and Δn = 0.2, indicates a required pitch significantly greater than 2.5 μm. Thus, at least for relatively low shear stress conditions, it appears that the liquid crystal layer performs as a reasonable wave guide. Hence, the intensity observed through the second polarizer will vary with $\sin^2\theta$, where θ is the director orientation at the fluid interface.

MEASUREMENTS IN LAMINAR DUCT FLOW

The nematic liquid crystal material used in the present investigation was supplied by Merek Ltd., England and was designated BL009. Previous surface shear stress investigations using nematic liquid crystal methods have been hampered by the low viscosity of the commonly available materials. In particular, full surface shear stress measurements using the rotation time technique were very difficult because of the video rate restriction. The viscosity

Downloaded From: http://proceedings.asmedigitalcollection.asme.org/ on 05/24/2018 Terms of Use: http://www.asme.org/about-asme/terms-of-use

of the BL009 material which is approximately 0.083 Pa.s, was further increased by adding a small amount of liquid crystal polymer (approximately 6.1 % by weight) giving a mixture viscosity of approximately 0.58 Pa.s. (The liquid crystal polymer was again supplied by Merek Ltd., and was designated LCP83.)

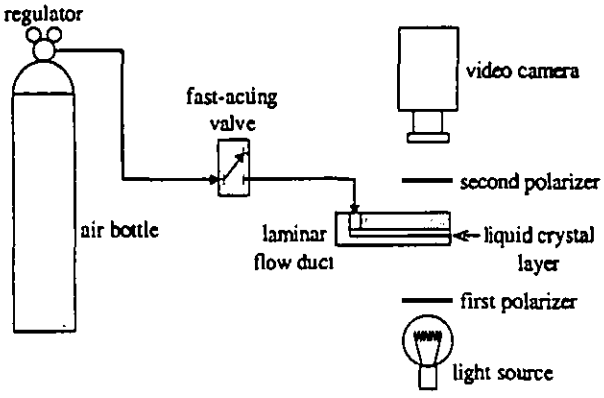

Figure 6. Diagram of the experimental arrangement.

To determine the validity of the mathematical model, measurements were obtained using the experimental arrangement shown in Figs. 6 and 7. The performance of the duct was investigated by monitoring the flow rate (using a rotameter) and taking pressure measurements at the locations shown in Fig. 7b. It was determined that there was fully developed laminar flow in the duct up to a Reynolds number (based on the duct height, a) of around 1000. (The critical Reynolds number for laminar flow in a circular pipe is usually quoted as 2000, e.g., Streeter and Wylie, 1981, p.239.) Theoretical laminar flow predictions based on solution of the two dimensional Poisson equation indicated that for the present geometry (a = 1 mm; b = 20 mm), the skin friction along the upper and lower surfaces will be accurately given by,

$$\tau_w = -\frac{a}{2}\frac{dp}{dx} \qquad (19)$$

provided $0.1 < z/b < 0.9$.

Measurements of the light intensity transmitted through the second polarizer (Fig. 6) were obtained at 27 different shear stress levels by recording the video signal and later extracting the intensity level using software developed by Wang et al. (1996). A measurement of intensity from a pixel of the video signal (corresponding to an area of approximately 0.02 mm^2), representing just one of the 27 shear stress levels, is presented in Fig. 8, along with results from the mathematical model. The location of this pixel was within the region $0.1 < z/b < 0.9$ (the uniform surface shear stress region of the duct). The measured values of intensity were normalized using the measured equilibrium orientation intensity at the maximum applied shear stress, which in the present example, was a value of almost 4 Pa.

For comparison with the experimental results, normalized intensity values from the mathematical model were obtained using the value of $\sin^2\theta$, where θ is the director orientation at the fluid

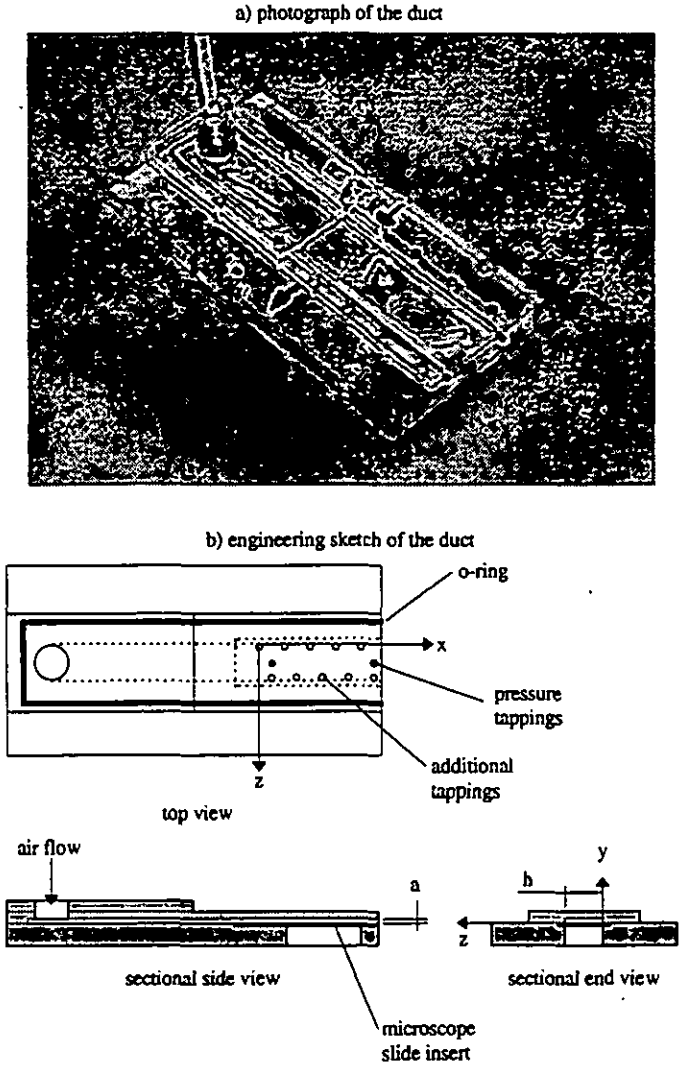

Figure 7. Illustration of the laminar flow duct.

interface. Further comparisons between the experimental results and the mathematical model are presented in Figs. 9 to 11 (using measurements from the same pixel used in Fig. 8). The appropriate scaling used to convert the mathematical model shear stress (C) into real units was determined by fitting the theoretical equilibrium orientation results to the experimental measurements, Fig. 9, and is given by,

$$\tau_w = 0.4C \qquad (20)$$

where τ_w is measured in Pascals. Similarly, the appropriate scaling for the rotation time was determined by fitting the theoretical flow-off relaxation time result to the experimental measurements, Fig. 10, and is given by,

$$t_{10-90} = 1.6T_{10-90} \qquad (21)$$

where $t_{10\text{-}90}$ is measured in seconds. (Note that rotation and relaxation times are now re-defined on the basis of a 10 % to 90 % rise time because experimentally, this is easier to determine than the

Downloaded From: http://proceedings.asmedigitalcollection.asme.org/ on 05/24/2018 Terms of Use: http://www.asme.org/about-asme/terms-of-use

time constant). Figure 11 compares the model for the flow-on rotation time with the experimental measurements, and uses the scaling factors determined from Figs. 9 and 10 to convert the theoretical result into real units. Thus, Fig. 11 provides a basis for an absolute comparison between the model and experimental results.

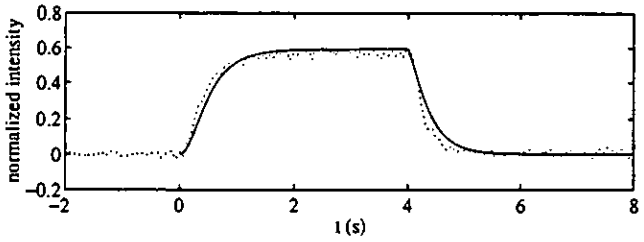

Figure 8. Comparison of measured intensity history (broken line) and theoretical prediction (solid line).

The trends predicted by the model in Figs. 9 and 10 were observed experimentally (it is inappropriate to compared the absolute levels since these experimental results were used to effectively calibrate the theoretical model). From Fig. 11, the correct trends were again predicted by the model, and furthermore, the absolute levels predicted by the theory compare favourably with the experimental results. (Figure 8, which also uses the scaling factors determined from Figs. 9 and 10, similarly demonstrates the high correlation which exists between the theoretical model and the experimental results.) It is therefore concluded that the mathematical model provides a good description of the physical processes associated with the nematic liquid crystal skin friction measurement techniques. Although the agreement between the experimental results and the theory is, on the whole, very good, it should be noted that at present, the model itself is not used to define the sensitivity of the shear stress measurement system. The actual sensitivity is determined using a curve fit to the calibration data. However, the real value of the model lies in the enhanced physical understanding which it provides. It is anticipated that the present mathematical model will aid future development and investigation of the measurement technique.

Further confirmation of the performance of the theoretical model is obtained by estimating the layer thickness using the scaling indicated by Eq. (21). Combining Eqs. (10) and (21) indicates that the layer thickness can be written,

$$l \approx \sqrt{\frac{1.6K}{\mu}} \qquad (27)$$

Assuming $K = 2.0 \times 10^{-11}$ N for the liquid crystal mixture (pure BL009 has elastic constants of $K_1 = 1.46 \times 10^{-11}$ N, and $K_3 = 2.99 \times 10^{-11}$ N), and $\mu = 0.58$ Pa.s (which is a bulk flow viscosity for the liquid crystal mixture) suggests a layer thickness of approximately 7.4 μm. This value is in acceptable agreement with the value of 10 μm which was estimated from measurements of the weight and the wetted surface area of the liquid crystal layer (assuming $\rho = 1000$ kg.m^{-3}).

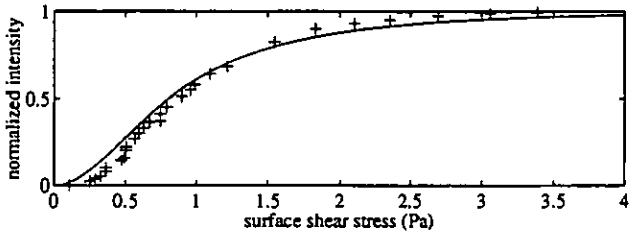

Figure 9. Comparison of measured equilibrium orientation (symbols) and theoretical prediction (solid line).

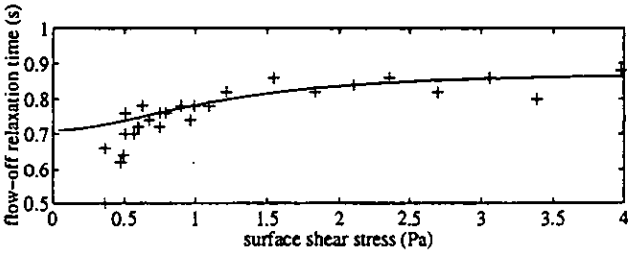

Figure 10. Comparison of measured flow-off relaxation time (symbols) and theoretical prediction (solid line).

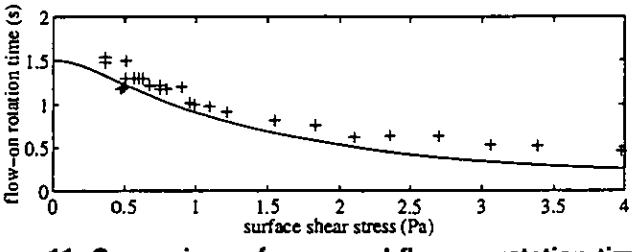

Figure 11. Comparison of measured flow-on rotation time (symbols) and theoretical prediction (solid line).

To determine the actual calibration of the nematic liquid crystal for the analysis of aerodynamic experiments using either the equilibrium orientation or rotation time techniques, it is possible to fit polynomials to the experimental calibration data (e.g., the experimental data presented in Figs. 9 and 11). For the equilibrium orientation data presented in Fig. 9, a second order polynomial was fitted (in a least squares sense) for $0.4 < \tau_w < 2$ Pa. Error estimates based on the deviation of the actual equilibrium orientation data from polynomial curve fit suggest that for any measured value of intensity, the uncertainty ($\pm 0.6745\sigma$) in the corresponding value of the surface shear stress is between ± 3 % and ± 4 % over this shear stress range. For the entire range of the rotation time data presented in Fig. 11, a 2nd order polynomial was fitted to a plot of τ_w versus $1/t_{10\text{-}90}$ (see Eq. 18). Error estimates suggest that the uncertainty of the surface shear stress measurements varies from ± 15 % at 1 Pa to ± 5 % at 4 Pa with the rotation time measurement technique.

FULL SURFACE MEASUREMENT DEMONSTRATION

As a demonstration of the full surface measurement capacity of the equilibrium orientation nematic liquid crystal technique

Downloaded From: http://proceedings.asmedigitalcollection.asme.org/ on 05/24/2018 Terms of Use: http://www.asme.org/about-asme/terms-of-use

developed here, a cylindrical obstruction was installed in the laminar duct as shown in Fig. 12. Prior to this experiment, every pixel in the uniform skin friction region of the liquid crystal layer ($0.1 < z/b < 0.9$) was calibrated using the unobstructed laminar flow duct (Fig. 7) at 7 different values of applied shear stress. The sensitivity at each of these points was determined (as discussed previously) by fitting a 2nd order polynomial to the calibration measurements (transmitted light intensity versus τ_w). At a flow rate of approximately 4.6×10^{-5} $m^3.s^{-1}$, the liquid crystal layer was allowed to reach its equilibrium orientation. The shear stress distribution was then determined from the measured equilibrium orientation intensity, and the prior calibration. Full surface shear stress results for this experiment are given in Fig. 13.

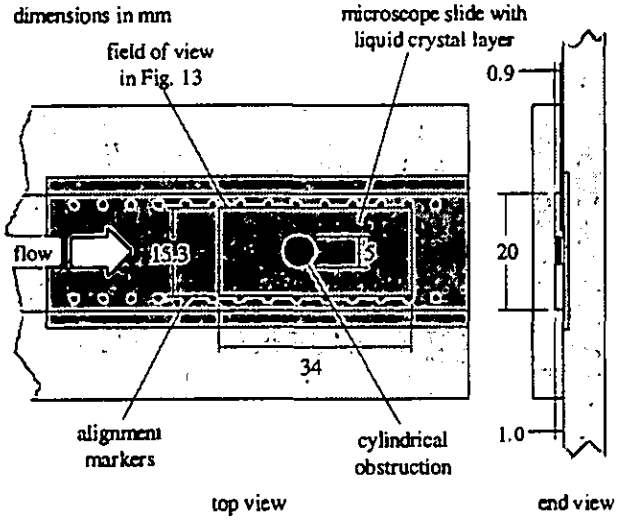

Figure 12. Laminar flow duct configuration for the cylindrical obstruction experiments.

Immediately ahead of the obstruction the surface shear stress is relatively low due to the deceleration of the flow as it approaches the obstruction. To negotiate a path around the obstruction, the flow accelerates, and thus generates regions of high surface shear stress on either side of the obstacle. Downstream of the obstacle, an extensive wake region is clearly apparent. However, *immediately* downstream of the cylinder, a small region of relatively high shear stress appears lo shadow it's circumference. This region has probably arisen due to the flow between the obstacle and the liquid crystal layer (the cylinder did not fully extend across the duct height - see Fig. 12). Clearly, the flow field is significantly different from that of a simple two-dimensional flow around a cylinder, as is further evidence by the regions of high shear stress that bound the wake flow region. However, the experiment was not conducted with the intention of performing an in-depth analysis of this particular flow field. Rather, the experiment is presented simply as a demonstration of the technique's potential.

The cylindrical obstruction was placed centrally within the width of the duct. It is therefore reasonable to expect the observed flow field to be symmetrical. The primary features of the flow field are indeed largely symmetrical, however, there remain a number of localized features that are not symmetrical (e.g., the apparent localized high shear stress values ahead of the obstruction). In these regions, the response of the liquid crystal did not follow the assumed second order polynomial calibration. Such features are caused by nonuniformities within the layer due to contamination of the layer with dust particles, and imperfection in the production of the liquid crystal layer. However, application of the technique in an unfiltered flow does not necessarily represent a particular difficulty, since the contamination will be localized and thus, only a small fraction of the data cannot be used. A similar argument can be applied to flaws arising in to the production of the layer, however, it should be possible to avoid such imperfections - techniques to improve the uniformity of the layer are currently being investigated.

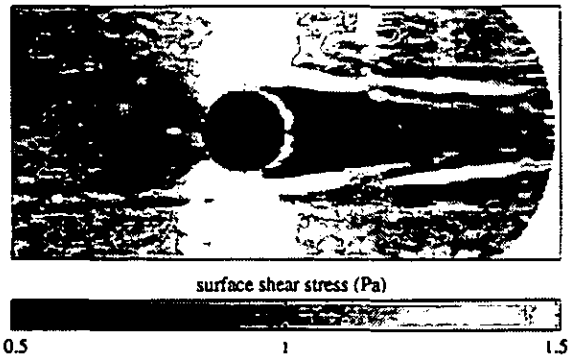

Figure 13. Full surface skin friction distribution around the cylindrical obstruction.

In the region ahead of the cylinder, the flow direction may deviate significantly from the general flow direction and may even approach the initial orientation of the liquid crystal director. In such regions, the flow direction will have a strong influence on the magnitude of the results. Such effects have not yet been incorporated into the analysis of the intensity measurements, and therefore the quantitative validity of the measurements (Fig. 13) in this region is somewhat doubtful. Future work will include an investigation of the flow direction sensitivity of these nematic liquid crystal techniques, with a view to the development of a simple technique for full surface skin friction vector measurements.

CONCLUSIONS

It has been demonstrated that direct full surface skin friction measurements are possible with simple techniques based on the use of nematic liquid crystal. With nematic liquid crystal, direct surface shear stress measurements can be obtained using either a rotation time technique or an equilibrium orientation technique. Both of these nematic liquid crystal techniques differ significantly from the colour change approach of Reda et al. (1996) in that the measured intensity of polarized light transmitted through the layer is calibrated to determine the surface shear stress.

Downloaded From: http://proceedings.asmedigitalcollection.asme.org/ on 05/24/2018 Terms of Use: http://www.asme.org/about-asme/terms-of-use

When a shear stress is applied to the nematic liquid crystal layer, the layer begins to flow in the direction of the applied shear. However, calculations indicate that for the viscosity and thickness of the present layers, the downstream migration will have a negligible influence on the measurements. A theoretical model for the molecular rotation dynamics has been introduced. Through comparison of the theoretical model and the present experimental measurements, it is demonstrated that the model provides a very good description of the physical layer behaviour. Future assessment, development, and application of the technique will by aided by the mathematical model. The present techniques are directly sensitive to the surface shear stress, however, the viscosity of the liquid crystal is also temperature sensitive and hence, the measurement techniques are ideally applied in isothermal flows.

Based on the deviation of the nematic liquid crystal calibration results from the least squares polynomial curve fits which were applied to the data, it is estimated that direct surface shear stress measurements can be made to within ± 4 % using the present techniques. Thus, the techniques developed here offer the considerable advantage of simplicity, but do not compromise the measurement accuracy relative to other surface shear stress measurement techniques. Following the full surface calibration of the liquid crystal layer, a cylindrical obstruction was placed in the laminar flow duct. The skin friction distribution was visualized with video imaging and then quantitative full surface shear stresses were determined using the calibration data. These measurements represent the first full surface skin friction measurements using the equilibrium orientation nematic liquid crystal technique.

Future work includes the investigation of materials with higher viscosities and elastic constants so that regimes of higher skin friction can be accessed using the present techniques. (The maximum shear stress used in the present investigation of the liquid crystal layer was approximately 4 Pa). At present, skin friction measurements are made using a light transmission arrangement, however it is also intended to develop the technique so that the liquid crystal layer can be viewed in reflection. A full surface shear stress vector measurement technique (i.e., giving the magnitude of the shear stress and the local flow direction at the surface) can be developed through the simultaneous use of the equilibrium orientation and the rotation time techniques.

REFERENCES

Bandyopadhyay, P. R., and Weinstein, L. M., 1991, "A Reflection-Type Oil-Film Skin-Friction Meter," *Experiments in Fluids*, Vol. 11, 281-292.

Bonnet, P., Jones, T. V., and McDonnel, D. G., 1989, "Shear-Stress Measurement in Aerodynamic Testing Using Cholesteric Liquid Crystals," *Liquid Crystals*, Vol. 6, No. 3, 271-280.

Carslaw, H. S., and Jaeger, J. C., 1959, "Conduction of Heat in Solids," 2nd ed., Oxford University Press.

Fernholz, H. H., Janke, G., Schober, M., Wagner, P. M., and Warnack, D., 1996, "New Developments and Applications of Skin-Friction Measuring Techniques," *Meas. Sci. Technol.*, Vol. 7, 1396-1409.

Hanratty, T. J., and Campbell, J. A., 1996, "Measurement of Wall Shear Stress," in R. J. Goldstein (Ed.), *Fluid Mechanics Measurements*, 2nd ed., Taylor and Francis, Washington D.C., pp. 575-648.

Jones, T. V., 1992, "The Use of Liquid Crystals in Aerodynamic and Heat Transfer Testing," in J. A. Reizes (Ed.), *Transport Phenomena in Heat and Mass Transfer*, Vol. 2, Elsevier, Amsterdam, pp. 1242-1273.

Jones, T. V., and Walton, T. W., 1991, "Reynolds Analogy in Film Cooling," 10th Int. Symp. on Air Breathing Engines, pp. 1263-1268.

Marshakov, A. V., Schetz, J. A., Kiss, T., 1996, "Direct Measurement of Skin Friction in a Turbine Cascade," *J. Propulsion and Power*, Vol. 12, No. 2, 245-249.

Reda, D. C., Muratore, J. J., and Heineck, J. T., 1994, "Time and Flow-Direction Responses of Shear-Stress-Sensitive Liquid Crystal Coatings," *AIAA J.*, Vol. 32, No. 4, 693-700.

Reda, D. C., and Muratore, J. J., 1994, "Measurement of Shear Stress Vectors Using Liquid Crystal Coatings," *AIAA J.*, Vol. 32, No. 8, 1576-1582.

Reda, D. C., Wilder, M. C., Farina, D. J., Zilliac, G., McCabe, R. K., Lehman, J. R., Hu, K. C., Whitney, D. J., Deardorff, D. G., 1996, "Areal Measurements of Surface Shear Stress Vector Distributions Using Liquid Crystal Coatings," AIAA Paper 96-0420.

Streeter, V. L., and Wylie, E. B., 1981, "Fluid Mechanics," 1st SI metric edition, McGraw-Hill, Singapore.

Tanner, L. H., and Blows, L. G., 1976, "A Study of the Motion of Oil Films on Surfaces in Air Flow, with Application to the Measurement of Skin Friction," *J. Physics E: Sci. Instr.*, Vol. 9, No. 3, 194-202.

Walton, T. W., 1990, "Shear Induced Twist in Nematic Liquid Crystals," Department of Engineering Science Report, University of Oxford, April, 1990.

Wang, Z, Ireland, P. T., Jones, T. V., and Davenport, R., 1996, "A Colour Image Processing System for Transient Liquid Crystal Heat Transfer Experiments," *J. Turbomachinery*, Vol. 118, No. 3, 421-432.

White, F. M., 1991, "Viscous Fluid Flow," 2nd ed., McGraw-Hill, New York.

Winter, K. G., 1977, "An Outline of Techniques Available for the Measurement of Skin Friction in Turbulent Boundary Layers," *Prog. Aerospace Sci.*, Vol. 18, 1-57.

Downloaded From: http://proceedings.asmedigitalcollection.asme.org/ on 05/24/2018 Terms of Use: http://www.asme.org/about-asme/terms-of-use